Condensation nuclei and aerosol optical depth measurements through the western Pacific Ocean

A. M. Bromley[1], M.J. Harvey[1], S. A. Gray[1] and J. McGregor[1]

[1] *National Institute of Water and Atmospheric Research (NIWA), Private Bag 14901, Wellington, New Zealand*

Correspondence: *Tony.Bromley@niwa.co.nz*

Key words: condensation nuclei, aerosol optical depth, western Pacific Ocean, aerosol source regions, back trajectories

Abstract

We present observations of condensation nuclei (CN) and aerosol optical depth (AOD) from a shipboard project using bulk-carrier ships sailing through the western Pacific Ocean between Nelson, New Zealand, and Osaka, Japan. The data is from eight voyages between 2006 and 2013.

CN counts for all voyages followed the same broad pattern: highly variable numbers near New Zealand, then variable and occasionally very high counts north of New Zealand through to the South Pacific Convergence Zone (SPCZ) and the Intertropical Convergence Zone (ITCZ). Through the north western Pacific Ocean there were generally very low counts until approaching Japan when high counts were measured in eastward outflow from Japan, Korea and China.

AOD measurements were made on voyages from 2007 at 20- minute intervals during daylight hours when the sun was clear of cloud. Back trajectories were calculated to identify airmass source regions. The AOD data were plotted in relation to the identified source regions to give estimates of aerosol size and turbidity. The AOD data was then compared to aerosol information obtained from the Moderate Resolution Imaging Spectroradiometer (MODIS) instrument onboard the Aqua earth-orbiting spacecraft.

Substantial temporal variability in fine spatial structure of the latitudinal occurrence of CN and AOD was noted. This often reflected the position and strength of the major convergence zones and the movement of synoptic-scale weather systems through the western Pacific Ocean. The aerosol data matches well with the source regions identified by back-trajectory plots. The variability in transport may be as important as variability in sources in determining the structure of CN across the western Pacific Ocean.

1. Introduction

From 2006 to 2013 measurements of condensation nuclei (CN) were made aboard MV Transfuture5, operated by the Toyofuji Shipping Company based in Nagoya, Japan. The ship sailed through the western Pacific Ocean on direct voyages between Nelson, New Zealand (41° 17' S; 174° 17' E) and Osaka, Japan (34° 40' N; 135° 30' E) at an average speed of 37 km h^{-1}. The voyage of 10,000km is completed in just under 12 days on a great circle transect

Submitted: 19 July 2018
Accepted: 28 November 2018

that runs approximately north-south across the South Pacific Convergence Zone (SPCZ) and Intertropical Convergence Zone (ITCZ). The individual voyage tracks are spatially identical, generally varying no more than 5km at any location. On the voyages from 2007 onwards shipborne aerosol optical depth data were also collected during daylight hours when the sun was clear of cloud.

Atmospheric aerosols are one of the largest sources of uncertainty in the current understanding of climate change (IPCC, 2013). They affect the climate by absorbing and scattering solar radiation (direct radiative effect), acting as cloud condensation nuclei (CCN) and hence affecting the radiative properties of clouds (indirect radiative effect). Chemical changes can occur on aerosol surfaces, altering the chemical and radiative properties of the atmosphere. Aerosol sources include biomass burning, volcanic eruptions, sea salt, biological and fossil fuel burning and aeolian dust. A secondary aerosol source originates with gas-to-particle conversion from the oxidation of organic and inorganic gaseous compounds (de Leeuw et al., 2014). A summary of aerosol data collected around the Pacific basin as part of numerous field experiments – GLOBE (Global Backscatter Experiment), ACE-1 (First Aerosol Characterisation Experiment), PEM A & B (Pacific Exploratory Mission) – has been published by Clarke et al., 2001, with emphasis on new particle production and evolution.

Quantifying the size distribution and chemical composition of aerosols is critical for estimating their impact on climate. The relatively short life-times of atmospheric aerosols and large spatial differences makes it difficult to relate the few surface-based observations to regional scales. Estimates of direct and indirect aerosol radiative effects are poorly constrained by observations, particularly in marine regions. Here, the clouds are susceptible to anthropogenic effects and the potential for indirect aerosol radiative forcing is largest.

Oceans constitute one of the single largest sources of atmospheric aerosols. Estimates have shown that around 30% of the total natural aerosol flux to the atmosphere is of marine origin and in the range of 1000 to 2000 Tg per year (Prospero et al., 1983; Andreae, 1995). Marine aerosols have two main components: primary aerosols produced over the sea surface by breaking bubbles and whitecaps, and the secondary non-sea-salt (nss) aerosols produced mostly by the chemical decomposition of dimethyl sulfide (DMS) and other organics produced by marine phytoplankton. Sub-micrometre aerosols form CCN in marine stratocumulus clouds (Charlson et al., 1987), influence the droplet size distribution and cloud albedo, and affect the visibility in the atmosphere over oceans (Fitzgerald, 1991). Mineral aerosols from continental and arid regions are also transported by winds to remote ocean locations and can be a source of trace minerals that support marine phytoplankton (Hoppel et al., 1990, Martino et al., 2014).

The western Pacific Ocean is a large ocean area that is influenced by all sources of aerosol production and transport: wave and bubble production, secondary aerosol production (especially in the southern western Pacific, an area of rich biological activity) and long-range atmospheric transport of aerosols from Australia, Indonesia and continental Asia. However, there are few in situ aerosol data for the region.

Here we explore the spatial distribution and transport using CN data collected during eight ship voyages between New Zealand and Japan and investigate likely aerosol source regions by long-range back trajectory calculations. In addition, AOD measurements were taken during daylight hours with clear sky conditions. We describe the measurement techniques specific to this study, followed by a discussion of the general meteorology through the western Pacific Ocean. The data from each of the transects are presented and detailed local meteorology is used to interpret various features of the CN data on each of the

eight voyages. We examine the data to determine if there is evidence of patterns suggestive of different populations of aerosols. We also discuss the large variations and interannual changes in the latitudinal distributions of CN and investigate the relationship with meteorological patterns.

2. Meteorological overview and aerosol climatology of the western Pacific

The atmospheric climatology of the Pacific Ocean and transportation of aerosols has been described by several researchers (e.g. Merrill, 1989; Prospero et al., 1989). The main meteorological features of the Pacific Ocean are shown in Figure 1. Complex tropical meteorology plays a major role in seasonal and latitudinal variations of aerosol content in the western Pacific lower troposphere. (Merrill et al, 1997). Observations have shown that the spatial variation in tropospheric aerosol over the equatorial western Pacific is related to the locations of the Intertropical Convergence Zone (ITCZ) and the South Pacific Convergence Zone (SPCZ) (Zaizen et al., 1996). The merger of moisture-laden trade winds in the tropical Pacific leads to the formation of the convergence zones (Vincent, 1994; Merrill et al., 1989). The ITCZ is the most persistent, lying between 2° - 12°N and crossing the breadth of the Pacific from Asia to Central America. It forms a strong barrier to direct inter-hemispheric transport. The ITCZ and SPCZ merge together in the western Pacific in the area 140°- 160°E, but separate further east with the SPCZ extending southeast towards Samoa and Tonga, and finally weakening and disappearing over the open South Pacific Ocean in the region of Easter Island (Figure 1). This constitutes a zone where two contrasting air masses (one originating from Southern Hemisphere ocean areas, the other prone to influence from a major continental landmass) meet and are mixed and carried high into the troposphere by strong convection. An extensive review of the behaviour and meteorology of the SPCZ has been published by Vincent (1994), who reports that its position and intensity vary seasonally but it is much more active and farther south in the summer months (December – February).

The summer southward shift of the SPCZ and an area known as the Subtropical Pacific High results in a

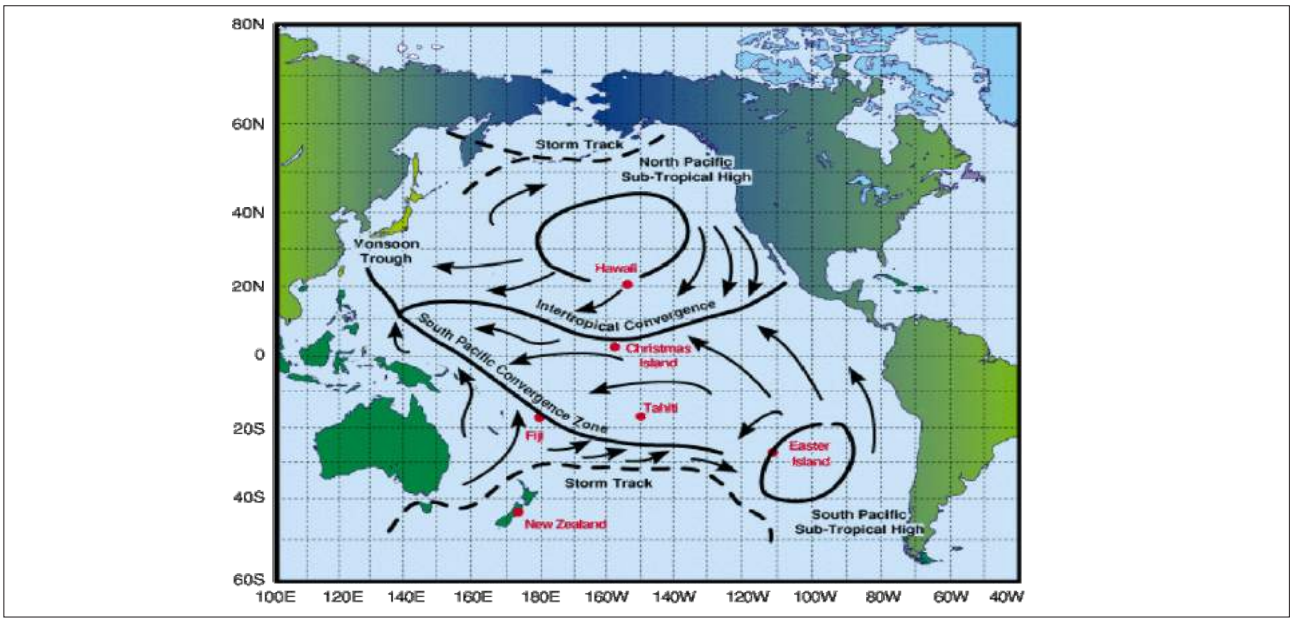

Figure 1: Main meteorological features of the Pacific Ocean (courtesy of NASA PEM-Tropics campaign).

broad region of convergence over northern Australia and eastward into the Pacific towards the Solomon Islands, producing extensive convective activity. The constant deep convection and high precipitation rates associated with the convergence zones makes accurate back-trajectory analysis difficult once the wind enters a convergence zone (Merrill, 1989). The SPCZ forms a weaker barrier to inter-hemispheric transport than the ITCZ and fluctuates seasonally in strength with major circulation changes associated with El Niño Southern Oscillation (ENSO) events. Atmospheric transport paths in the western South Pacific are less well understood than those in the North Pacific.

Southeast trade winds dominate the area north of New Zealand to 20°S and westerly winds occur on the southern side of the high-pressure belt near southern New Zealand. In winter the SPCZ migrates north and east, and south-east trade winds cover most of the southwest Pacific north of New Zealand, and westerly winds dominate between the Subtropical Pacific High and the Southern Ocean areas to the south.

North of the equator the meteorology of the lower atmosphere is dominated by two major meteorological systems in the region: the Pacific High and the Japan Jet (Merrill et al.,1997). The Japan Jet tends to be weaker and farther north in the late Northern Hemisphere summer and early autumn. During the summer/autumn period the Pacific High tends to be located more to the east and north, impeding outflow from continental Asia and enhancing the low-level flow of marine and Southern Hemisphere air into the northern mid-tropical latitudes. The northern spring period is characterised by maximum outflow from Asia, entraining emissions from the continent within a westerly flow out over the north Pacific. This flow can then swing southwards and move around the North Pacific High and bring Asian emissions into the tropical central Pacific through the northeast trade wind flows (Merrill, 1989).

In the southwest Pacific the dominant sources of aerosol mass are dust blown from the Australian continent and nss sub-micrometre aerosols produced from dimethyl sulfide (DMS) oxidation once emitted into the atmosphere following the production of precursor dimethylsulfoniopropionate by phytoplankton.

3. Shipboard sampling methodology

The Transfuture5 voyages are part of a regular trade route from the port of Nelson, New Zealand travelling directly to Osaka, Japan on a bearing of 349°T, with only a brief deviation between New Britain and Bougainville in the Solomon Islands. Each voyage was completed in 11.5 days. Although the aerosol data were collected from the commencement of the voyage, this paper discusses only the data from 30°S northwards. The data collected through the Tasman Sea off the west coast of New Zealand's North Island will be the subject of a separate paper.

NIWA's air sampling on Transfuture5 was centred on a steel shipping container attached to the top deck (deck 13). The container is located centrally, 70m from the bow and 20m aft of the crews' quarters and bridge complex. It is 100m forward of the ship's engine exhaust stack. NIWA collected the data as part of the Ships of Opportunity (SOOP) programme of the Centre for Global Environment Research of Japan's National Institute for Environmental Studies (NIES) led by Dr Y. Nojiri (Nara et al., 2011).

A TSI model 3010 condensation particle counter (CPC) sampled and counted sub-micrometre particles (>10 nm diam.) on a continuous basis. It has an upper concentration of 10,000 particles cm^3 and responds quickly to concentration changes. The CPC passes air through a heated alcohol reservoir where n-butyl alcohol condenses onto particles in the sample flow creating aerosol droplets large enough to be detected using a light-scattering technique. The sample passes into a vertical condenser tube cooled by a thermoelectric heat pump.

Here the alcohol vapour supersaturates and condenses onto virtually all particles larger than 10 nanometres in diameter, regardless of chemical composition. As droplets exit the condenser they pass through a thin ribbon of laser light. Light scattered by these droplets is collected by optics and focussed onto a photodetector which converts the light signal to an electric pulse which is recorded as a particle count.

Although the CPC is ideal for measuring very low particle concentrations, it is capable of detecting concentrations greater than 10,000 particles cm^3. The limiting factor is coincidence. The CPC counts single particles, so that each particle scatters a separate pulse of light. At high concentrations two or more particles can be in the viewing volume at the same time: the pulses they generate overlap and are counted as one particle. The frequency of this event depends on particle concentration. Within limits it is possible to determine coincidence. The coincidence correction is important at very high concentrations, but for most of the measuring range the coincidence effect is negligible. The actual particle concentration can be calculated by:

$$N_a = N_{i\,exp} (N_a QT)$$

Where N_a = actual concentration (particles cm^3)

N_i = indicated concentration (particles cm^3)

Q = 16.67 cm^3/s

T = 0.4 microsecond (the effective time each particle is in the viewing volume)

The N_a exponent can be approximated by N_i

The following table shows the calculated coincidence for a range of concentrations. Coincidence is $1-N_a / N_i$

Table 1: Calculated coincidence versus particle concentration.

Concentration (particles cm^3)	Calculated coincidence (%)
10	<0.01
100	0.07
1,000	0.67
5,000	3.5
10,000	7.4

During the voyages indicated concentrations in excess of 30,000 particles cm^3 were measured, especially just north of New Zealand. Although the actual number cannot be regarded as accurate because of high levels of coincidence, it does indicate the presence of very high particle concentration, well in excess of 10,000 particles cm^3.

The sampling intake was via a 5m ¼ inch copper tube; the inlet was located 2m above the bow end of the NIWA sampling room. The flow rate was controlled by a critical orifice with a flow rate of 1L min^{-1} and data were logged onto a computer as 30-second count accumulations. The CN concentrations were recorded as the number of particles per cm^3 of sampled air. There was no sector control used with the CPC as the intake was located 100m forward of the ship's funnel. The average speed of Transfuture5 was around 37km hr^{-1} and at this speed contamination by ship emissions was very rare and readily spotted during QC checks on the data after the voyage. In August 2006 a prolonged spell of strong south-south-east winds brought ship emissions from the engine exhaust over the CPC intake between 17.5°S and 5°S. These data have been excluded from the analysis. Occasional very short-lived periods of contamination occurred, usually of the order of one hour or less e.g. ship barbeque deck party, or lifeboat drill when combustion engines were tested. Again, these data have been excluded.

From May 2007, aerosol optical depth (AOD) data were

measured on-board Transfuture5 on all voyages as a contribution to the Maritime Aerosol Network (MAN), (Smirnov et al., 2009, 2011), a maritime extension of the Aerosol Robotic Network (AERONET). Both AERONET and MAN provide high-quality aerosol information from several hundred individual locations distributed over the Earth's surface. Additionally, satellite remote sensing has the potential to complement these networks by providing fill-in coverage between surface measurement sites and, in the case of MAN, extended temporal coverage over the oceans.

The attenuation of solar radiation through the atmosphere is described by a version of the Beer-Lambert-Bouguer law as below:

$$I = I_0 \exp(-\tau\, m)$$

Here I_0 is the incident solar irradiance at the top of the atmosphere, I the irradiance at the ground, m is the airmass factor, dimensionless path length through the atmosphere, and τ, the optical thickness of the atmosphere. At normal incidence, τ is termed optical depth. Both m and τ contain contributions from a number of absorption and scattering mechanisms, including aerosols. The aerosol contribution to optical depth, τa', termed aerosol optical depth, may be deduced from ground-based measurements of irradiance by using the above equation and correcting for the known contributions from the remaining scattering and absorbing mechanisms.

Aerosol optical depth is wavelength dependent, and for the simple case of a unimodal log-normal aerosol particle size distribution, this wavelength dependence is well described by the Angstrom relation:

$$\tau(\lambda) = \beta\, \lambda^{-\epsilon x}$$

This power law relation is specified by the two parameters, the Angstrom turbidity, β, a wavelength independent measure of optical depth, and the Angstrom exponent, α, an inverse measure of particle size. For measurements of optical depth $\tau\lambda_1$ and $\tau\lambda_2$ respectively, the Angstrom exponent is given by:

$$\alpha = -\frac{\log \frac{\tau\lambda_1}{\tau\lambda_2}}{\log \frac{\lambda_1}{\lambda_2}}$$

The Angstrom exponent is inversely related to the average size of the particles in the aerosol: the smaller the particles, the larger the exponent. Thus, Angstrom exponent is a useful quantity to assess the dominant particle size of atmospheric aerosols.

The MAN aerosol measurements of column aerosol content were obtained with a Microtops handheld sunphotometer (Porter et al, 2001); measurements were made every 20 minutes during daylight hours when the sun was clear of cloud or if the cloud cover was even and very thin cirrus. (Note that in recent times the MAN network instructions have warned to avoid any sampling through thin cirrus cloud).

4. Results and discussion

Data from eight voyages along the same transect from 2006 to 2013 are described: two each during Southern Hemisphere winter and spring, three in autumn and one in summer.

Figures 2 to 5 (a) show graphically the CPC particle concentrations (30-second count accumulations averaged over 10 minutes), absolute wind speed, ambient air temperature, relative humidity, and sea-surface temperature for each voyage by season. Temperature, humidity and wind speed were measured at deck level, 47m above sea level. The schematic above the graphed data indicates true wind direction and amounts of high,

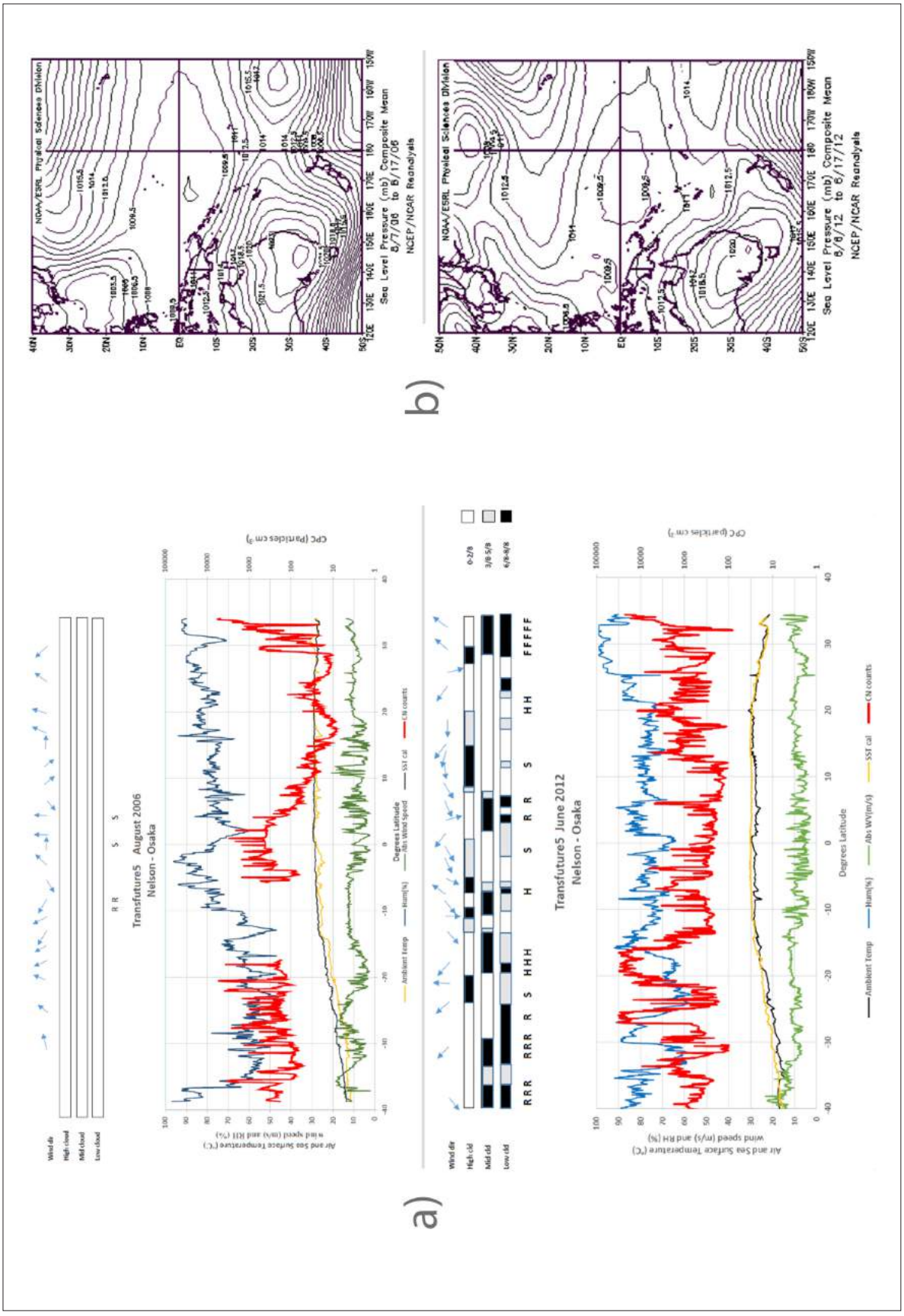

Figure 2: Winter voyages. (a) CPC particle concentrations (30-second count accumulations averaged over 10 minutes), absolute wind speed, ambient air temperature, relative humidity, and sea-surface temperature. (b) composite mean sea level (MSL) atmospheric pressure fields for each voyage by season.

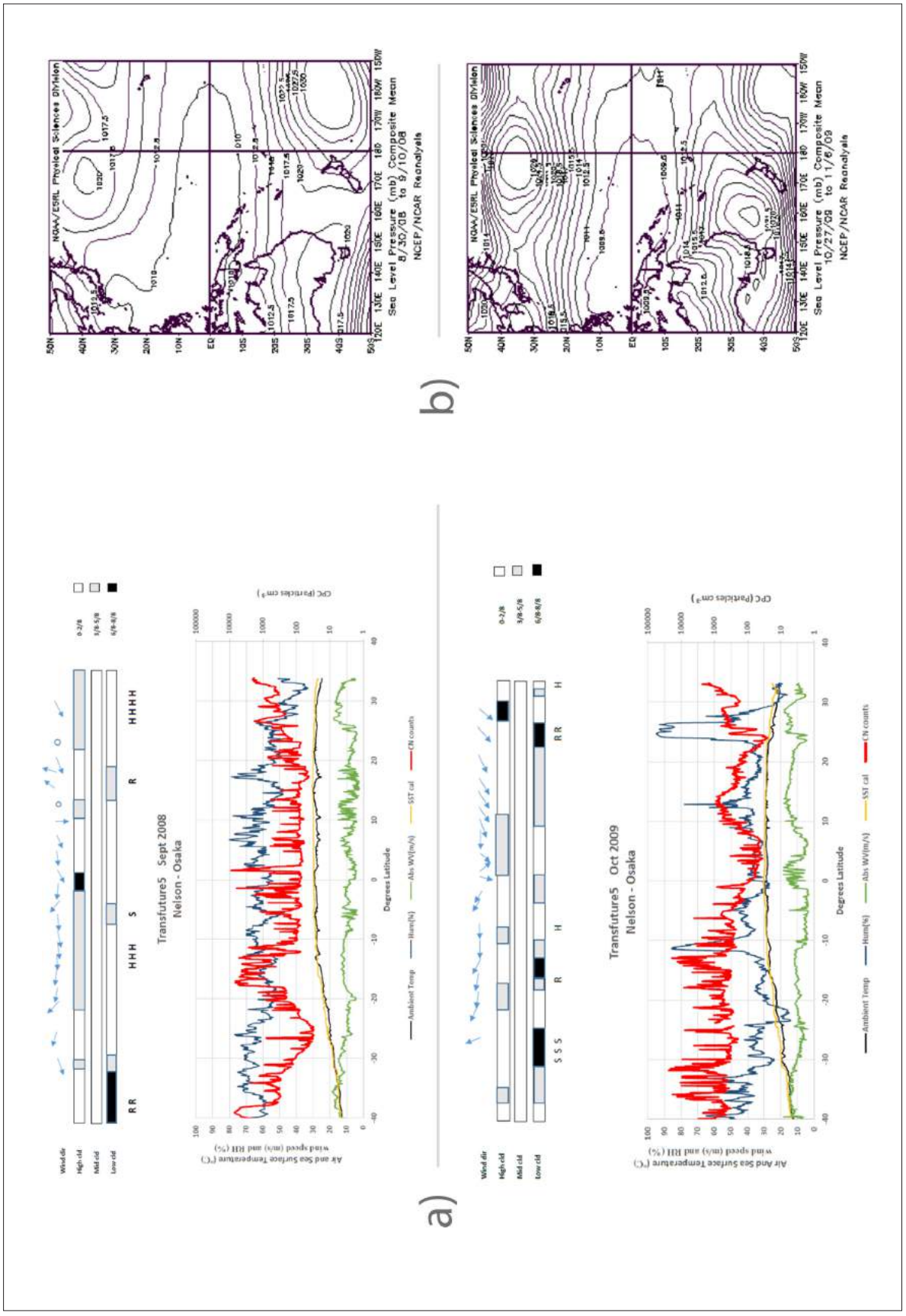

Figure 3: Spring voyages. (a) CPC particle concentrations (30-second count accumulations averaged over 10 minutes), absolute wind speed, ambient air temperature, relative humidity, and sea-surface temperature. (b) composite mean sea level (MSL) atmospheric pressure fields for each voyage by season.

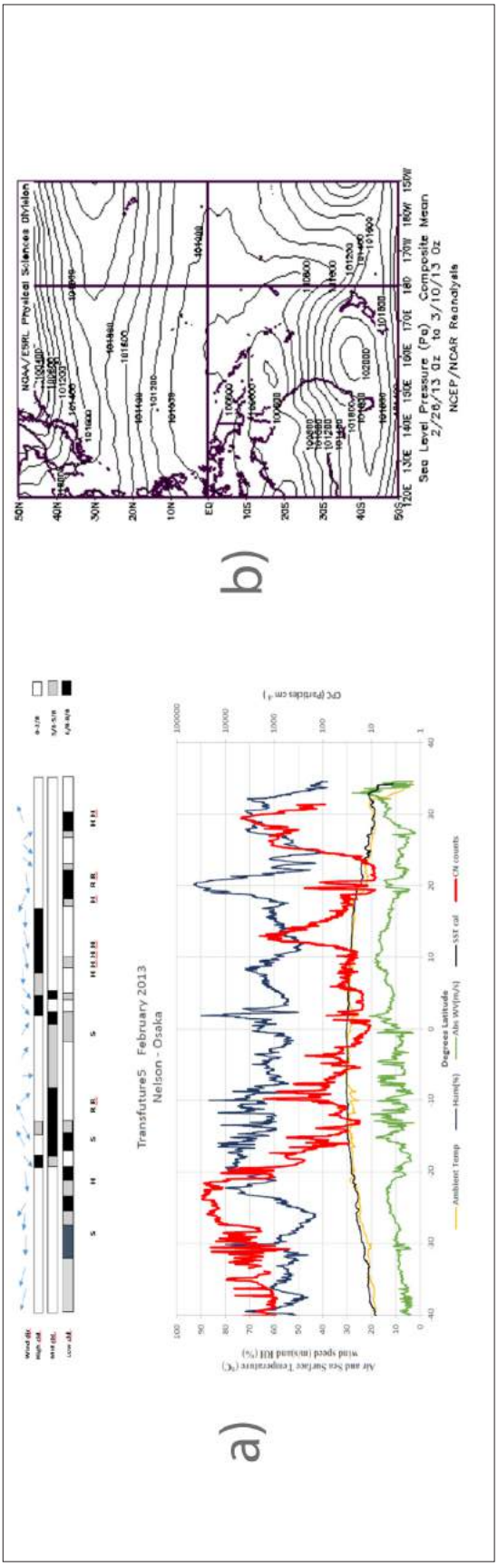

Figure 4: Summer voyages. (a) CPC particle concentrations (30-second count accumulations averaged over 10 minutes), absolute wind speed, ambient air temperature, relative humidity, and sea-surface temperature. (b) composite mean sea level (MSL) atmospheric pressure fields for each voyage by season.

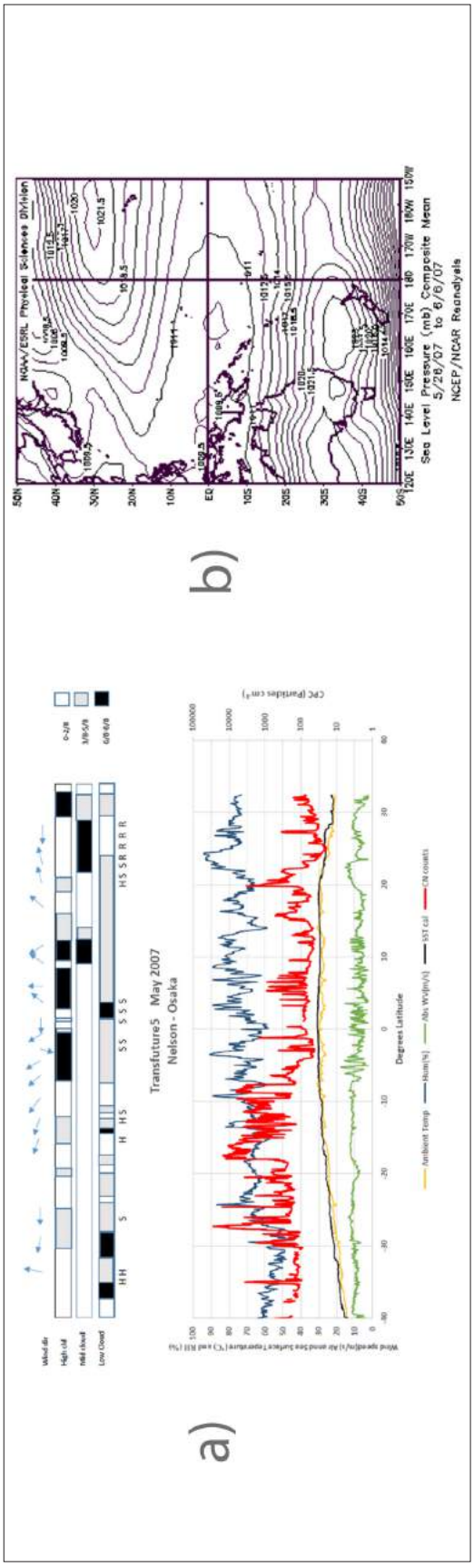

Figure 5: Autumn voyages. (a) CPC particle concentrations (30-second count accumulations averaged over 10 minutes), absolute wind speed, ambient air temperature, relative humidity, and sea-surface temperature. (b) composite mean sea level (MSL) atmospheric pressure fields for each voyage by season.

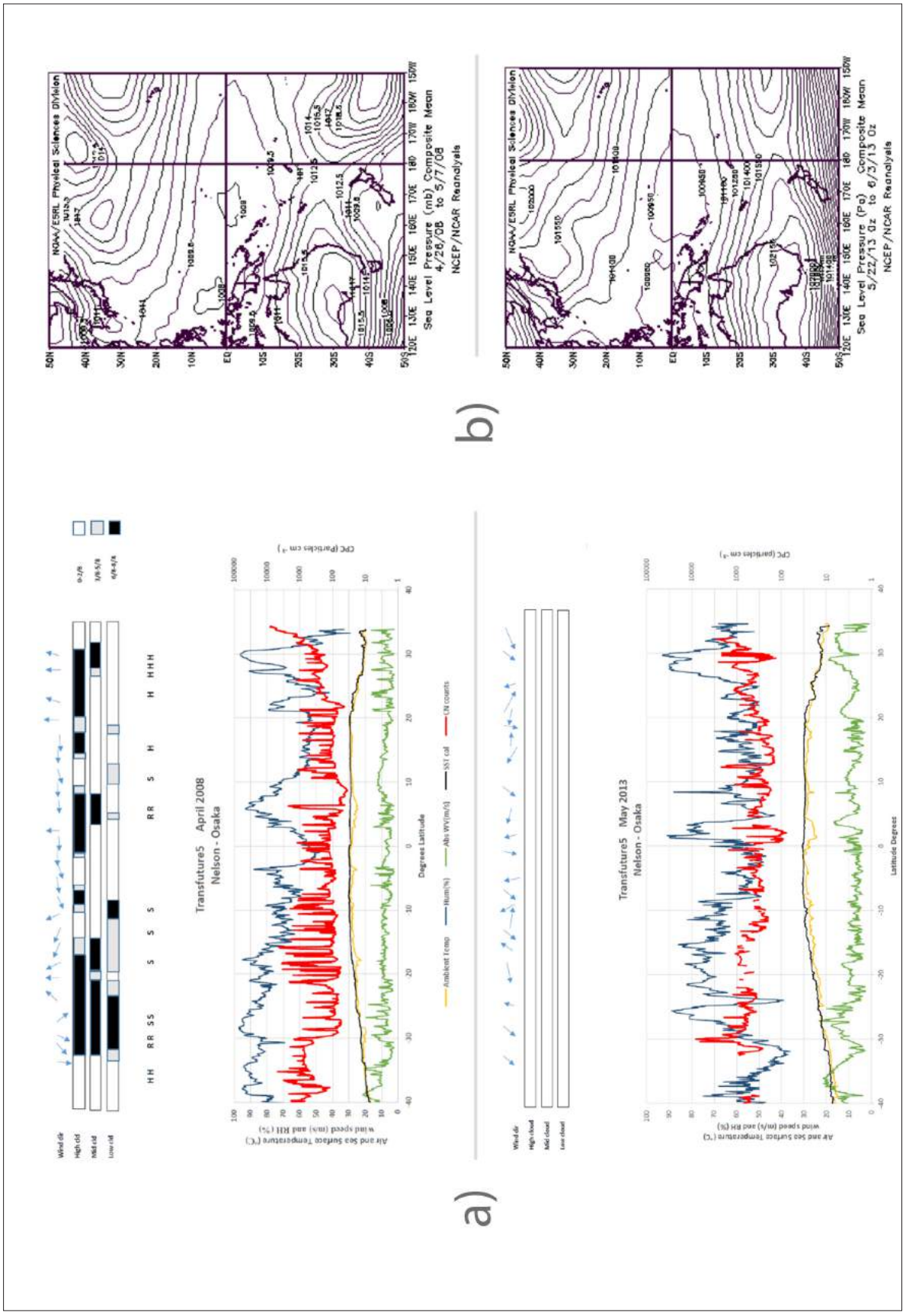

Figure 5 continued: Autumn voyages. (a) CPC particle concentrations (30-second count accumulations averaged over 10 minutes), absolute wind speed, ambient air temperature, relative humidity, and sea-surface temperature. (b) composite mean sea level (MSL) atmospheric pressure fields for each voyage by season.

middle and low cloud. Note that no cloud observations were recorded during voyages August 2006 and May 2013. The letters indicate occurrences of rain (R), showers (S), haze (H) and fog (F).

Figures 2 to 5 (b) show the composite mean sea level (MSL) atmospheric pressure fields for each voyage by season (Images provided by the NOAA/ESRL Physical Sciences Division, Boulder, Colorado from their Web site: http://www.esrl.noaa.gov/psd/) (Kainay et al., 1996). MSL patterns for each pairing of voyages are similar. Southern winter (August 2006, June 2012) has the Pacific High well to the north and east in the North Pacific, impeding outflow from Asia and bringing low-level oceanic air flow into the north-west Pacific region. Southern autumn (May 2007, April 2008) has the Pacific High in the central North Pacific, with stronger outflow from Asia into a westerly flow over the northern Pacific. Low-level oceanic flow on the southern side of the Pacific High brings easterlies into low northern hemisphere latitudes. Southern spring (September 2008, October 2009) has the sub-tropical jet stream (Japan Jet) further north and the Pacific High is still pushing a low-level oceanic flow onto eastern Asia. In all seasons, the area south of New Zealand is dominated by westerlies, while south-east trade winds cover the sub-tropical and tropical area north of New Zealand up to the region of the SPCZ.

CN counts for all voyages follow the same broad pattern: highly variable numbers in the vicinity of New Zealand, variable and occasionally high counts through the area north of New Zealand and up to the SPCZ and ITCZ. Relatively low but variable counts dominate around the convergence zones, followed by very low counts through the north-west Pacific where air has originated over low productivity / oligotrophic regions of the North Pacific Subtropical Gyre, before increasing again in the eastward outflow off Japan, Korea and China. An additional general observation was there was often an anti-correlation between CN number and high humidity excursions (April 2008, February 2013, May 2013). This phenomenon has been previously observed by McNaughton et al. (2004) in the boundary layer in Asian outflow and speculation is it could be due to the suppression of CN formation by higher surface area of coarse aerosol in high humidity, where they comment that "relative humidity approaching 100% appears to dramatically reduce the formation, growth and survival of the newly formed secondary aerosols."

The lowest counts (~10 cm^{-3}) were observed on the August 2006 and February 2013 voyages in air that had originated over the gyre region and was in or transported from the North Pacific Sub-Tropical High (Figure 1). By contrast, the June 2012 voyage was unusual in that there were consistently very high particle concentrations (>10,000 cm^{-3}) measured between 27°S and 13°S, which were thought to be due to a generally polluted airmass containing precursors and particles from industrial, and terrestrial emissions blowing off the Australian continent. Time series do also show many short duration spikes (e.g. June 2012) indicative of the occurrence of localised regions of nucleation and Aitken nuclei production. These were observed to occur downwind and in the proximity of islands with combustion and other anthropogenic activity and were often, not always absent in the northern end of the record (10° to 25°N) (e.g. see the contrast in August 2006, May 2007, October 2009). It is unlikely given the sample inlet placement but we cannot definitively exclude

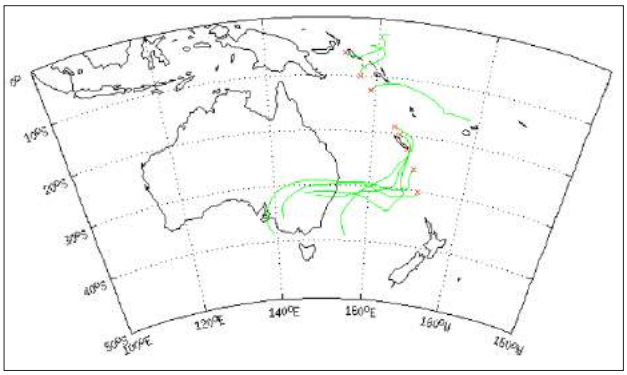

Figure 6: Back trajectory plots indicating transport of dust-laden air from SE Australia out into the western Pacific Ocean, June 2012.

local pollution of CN from the vessel as a source of some of the CN spikes. Figure 6 shows back trajectory plots indicating air measured at the ship at those latitudes had passed over southern and southeast Australia. A strong ridge of high pressure extended from Australia out over the Tasman Sea suppressing vertical mixing of the dust particles and allowing a concentrated plume to pass over the ship route north of New Zealand. Figure 13 shows AOD values associated with this air corresponding to mineral dust aerosols. Back trajectories from the May 2013 voyage (not plotted) also indicate an Australian source for the particle increase between 30.5°S and 29°S during that voyage.

4.1 Back trajectories

Air mass back-trajectories have been calculated for each voyage (HYSPLIT model via NOAA http://www.arl.noaa.gov/ready/hysplit4.html), (Draxler et al., 2003) using the Global Reanalysis 1948 – present data set as forcing meteorology to help identify the areas over which sampled air had passed. Ehhalt et al. (1999) calculated the range of residence times of tropospheric aerosols as a function of particle size (Figure 7). They point to an average CN residence time of 1-100 hours, so 4-day back trajectories were calculated.

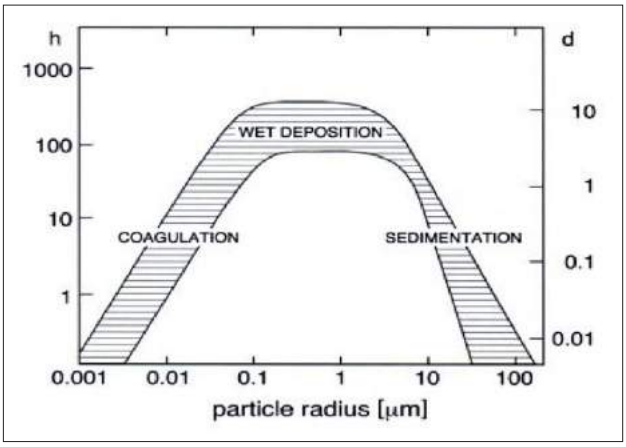

Figure 7: Range of tropospheric particle residence times (d=days, h=hours). The shaded bar shows typical range of lifetime between lower limit in the boundary-layer and upper limit at the tropopause versus size (after Ehhalt et al., 1999).

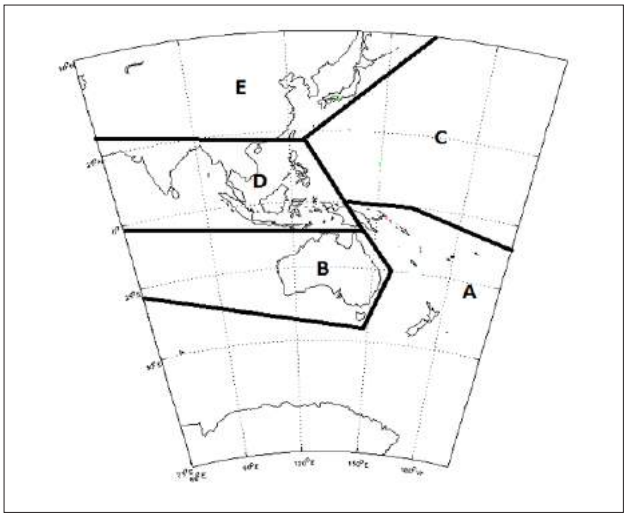

Figure 8: Airmass back trajectory region classification

We developed a system for identifying the origin of the sampled air mass: trajectory starting points were selected for times before, during and after any major change in recorded CN concentration. The trajectories were then used to classify the potential aerosol source regions. Five regions have been identified. The selected potential air mass origin classifications are shown in Figure 8.

Region A: Airflows that tend to follow the south-east trade wind regime in the South Pacific. This flow may also have spent many days over the Southern Ocean south of Australia and New Zealand before becoming entrained in the south-east trades flow.

Region B: Airflow directly from the Australian continent.

Region C: Westward airflow over the North Pacific Ocean towards south-east and continental Asia. These air masses have spent many days over open ocean but as mentioned earlier in the meteorological section, long-range transport of aerosols from Asian and North American sources can be entrained in this flow.

Region D: Outflow eastward into the North Pacific Ocean from Indonesia and Philippine Islands, with a likelihood of being influenced by industrial and domestic sources.

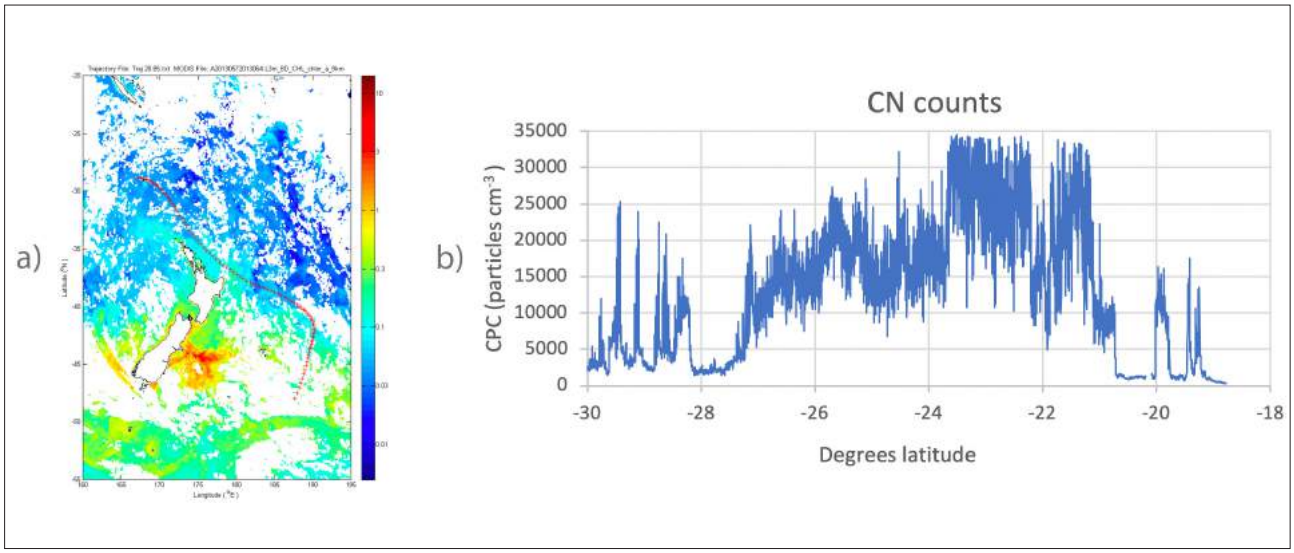

Figure 9: (a) MODIS 8-day chlorophyll-a with back trajectory plot as red dots, and (b) CN counts between 30°S and 19°S. February 2013 voyage.

Region E: Airflow associated with the eastward outflow off continental Asia, with the potential to be influenced by industrial and domestic emissions, and dust sources from the dry interior.

The airmass back trajectories at particular latitude bands are very similar for each voyage, the exception being August 2006 when surface winds north of the equator were westerlies off south-east Asia rather than the more common north-east or easterly trade winds from the central North Pacific Ocean. The air movements are consistent with the broad climatology of the Pacific described earlier and therefore representative of the region. The main airflows shown by the trajectories are similar to those found during the SEAREX programme (Merrill,1989).

Air from Region A (south-east trade winds) was encountered as far as the ITCZ, just north of the equator, and air from Region E (continental Asia) only north of 25°N. Flow from SE Asia was sampled only once, in August 2006.

4.2 Aerosol Characteristics of the source regions

Region A: This region is minimally impacted by transport of dust from continental sources. However very high particle counts in excess of 10,000 particles cm^3 have been measured just north of New Zealand on several of the voyages. These particles may well be correlated with particle formation associated with intense biogenic activity as the air passed over areas of ocean with active chlorophyll-a. VOC and DMS emissions from plankton in these areas are likely to enhance the particle concentration in the atmosphere.

In February 2013 a large spike of over 10,000 particles cm^3 in CN concentration was measured between 27°S and 21°S. MODIS satellite data showed chlorophyll-a and enhanced phytoplankton and biogeophysical chemistry activity around the New Zealand coast especially to the east of both main islands. Back trajectories showed the sampled air had travelled over an area of enhanced chlorophyll-a and it is likely the increase in CN concentration was a result of biogenic activity from this zone (Figure 9).

Another feature in most of the voyages was a CN spike in the region of 20°S. This has been attributed to particles produced by large scale open cast nickel mining in New Caledonia, and from the coal-fired power plants associated with the mining and smelting. Back trajectories indicate the sampled air had crossed the mining area before continuing out over the open ocean area. Figure 12 shows an example with trajectories indicating air passing over New Caledonia and the corresponding increase in CN between 13°S and 19°S as shown in Figure 3 September 2008 voyage data.

Some "spikiness" in the CN record occurs in the vicinity of the SPCZ and ITCZ. This is likely due to enhanced vertical motion associated with the zones, preventing extensive horizontal surface mixing of aerosols.

Region B: Australia is the major dust source in the South Pacific (Prospero et al., 1989, Martino et al., 2014). Large scale synoptic flows from Australia out into the SW Pacific are common. Much of Australia is arid, with over 4 million km^2 susceptible to severe dust storms (Loewe, 1943, Ekström et al., 2004, O'Loingsigh et al., 2017). On two voyages (June 2012 and May 2013) high concentrations of aerosols (in excess of 10,000 particles cm^3) were sampled that originated from the Australian continent. These plumes occurred in austral winter, which is the season of minimum dust activity on the Australian continent; this may imply that during the summer, when dust storm activity is more frequent, occurrences of aerosols originating from Australia may be much higher.

Region C: In general this part of the Western Pacific has low CN concentrations with prevailing winds from the easterly quarter. The air masses have had many days over open ocean and most anthropogenic sourced particles have either dropped out gravimetrically or washed out by rain. The northern spring period has maximum seasonal outflow from continental Asia, and these emissions can be entrained in this westerly flow, which can swing southwards over the eastern North Pacific and eventually move back westward into the central Pacific via the northeast trade wind flows (Merrill, 1989).

Regions D & E: These regions are densely populated areas with intensive industrial activity. Westerly flow off these regions out into the western Pacific Ocean will carry plumes of aerosols from a variety of urban and industrial sources. On the occasions the ship passed through these plumes, high CN counts were recorded. The high counts are associated with regular synoptic scale weather patterns.

4.3 Aerosol Optical Depth Measurements

Transfuture5 Microtops data are summarised in Figure 10. The Angstrom relation has been fitted to the AOD data for each sunphotometer measurement to reduce the multi-wavelength data to the two parameters, Angstrom turbidity, ß, and Angstrom component, α. For 440 to 870 nm wavelength range it gives useful discrimination of aerosol sources with values of order >2 indicating large fine mode – smoke, sulfates, 1.5 – 1.7 continental pollution, 0.4 – 0.6 maritime aerosol, and 0.0 – 0.4 mineral dust. When plotted in this two parameter ß - α space, some groupings and patterns in the data are evident, suggestive of different populations of air/aerosol being sampled. The sunphotometer data in Figure 10 is colour-coded according to source regions identified from the back trajectory calculations (Figure 8).

The most distinctive grouping is evident in the difference between air sourced from the Japan/mainland Asia region (red) affecting the western Pacific Ocean north of 20°N, and the air sourced from the two predominantly oceanic regions (blue and green). The Japan/Asia air has a combination of generally higher turbidity and higher Angstrom exponent, with the latter indicating a finer particle size. This is likely the result of dominant urban/industrial air pollution source.

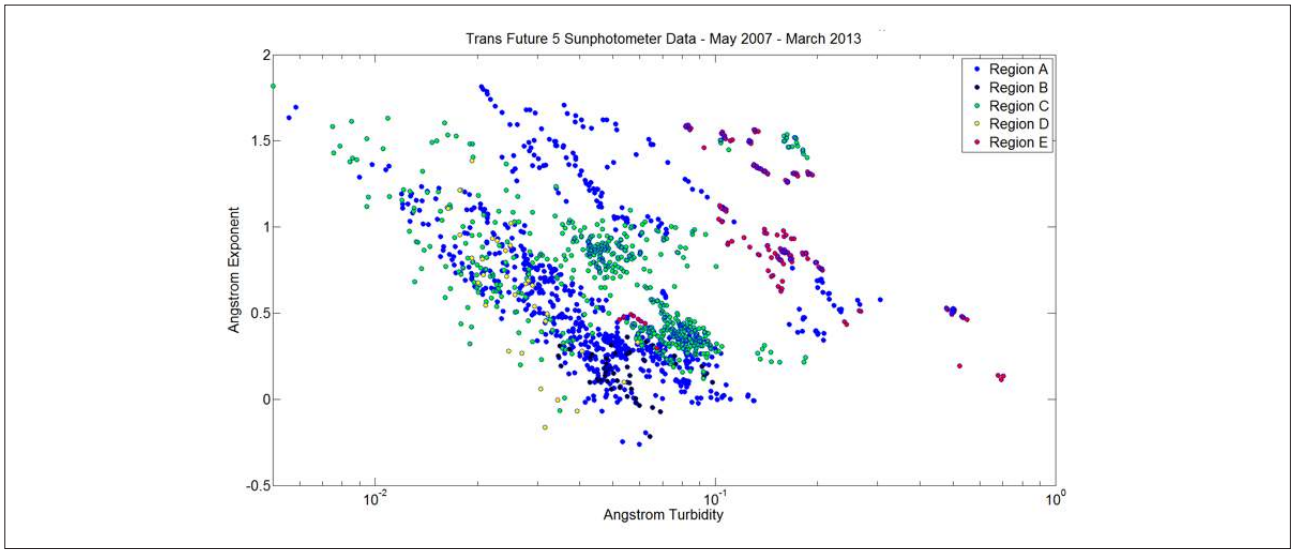

Figure 10: Combined AOD data from all voyages.

There is generally no clear distinction between sun photometer measurements of air sourced from the two oceanic regions (blue – south Western Pacific and Southern Ocean, and green – north Pacific). Both regions have similar β and α values, indicative of marine aerosol production.

In May 2007 however, there were two distinct groupings with some AOD data having abnormally high turbidity compared to the usual oceanic values (Figure 11a). Examination of the back trajectories for that voyage (Figure 11b) shows that some of the sampled air had previously passed over land regions a day or so earlier. From source region A (blue dots) some air had crossed over the Auckland area of New Zealand, the predominant urban region of that country; from source region C (green dots) air sampled near 25°N had crossed over Manila in the northern Philippines. The high turbidity AOD data is consistent with an interpretation of urban and industrial air pollution. In both cases a ridge of high pressure extending from the aerosol source region over the ship's track is likely to have suppressed the rate of particle dispersion and minimised rainout or washout, enabling a coherent plume to travel well out over the open ocean.

The September 2008 voyage AOD data shows two clearly defined groupings (Figure 12): oceanic air and air that has originated from China and Japan. Back trajectories show sampled air between New Zealand and 25°N (regions A & C) had been residing over open ocean for many days before coinciding with the ship's track (Figure 12b). The sunphotometer data show values of Angstrom turbidity and exponent that are typical of clean ocean air, in the main uncontaminated by anthropogenic sources. The data from the northwest Pacific region have a generally higher exponent value than that measured over the southern Western Pacific region (region A). North of 25°N sampled air had passed over densely populated and industrial areas of Japan and China with higher turbidity and exponent values, typical of urban/industrial pollution.

Figure 13 shows AOD data from the June 2012 voyage. A distinct grouping (circled) is associated with mineral dust particles, the sampled air having passed over south-eastern Australia as described earlier (see Figure 6).

4.4 Satellite – Transfuture5 AOD intercomparison

Satellite sensed aerosol information was obtained from

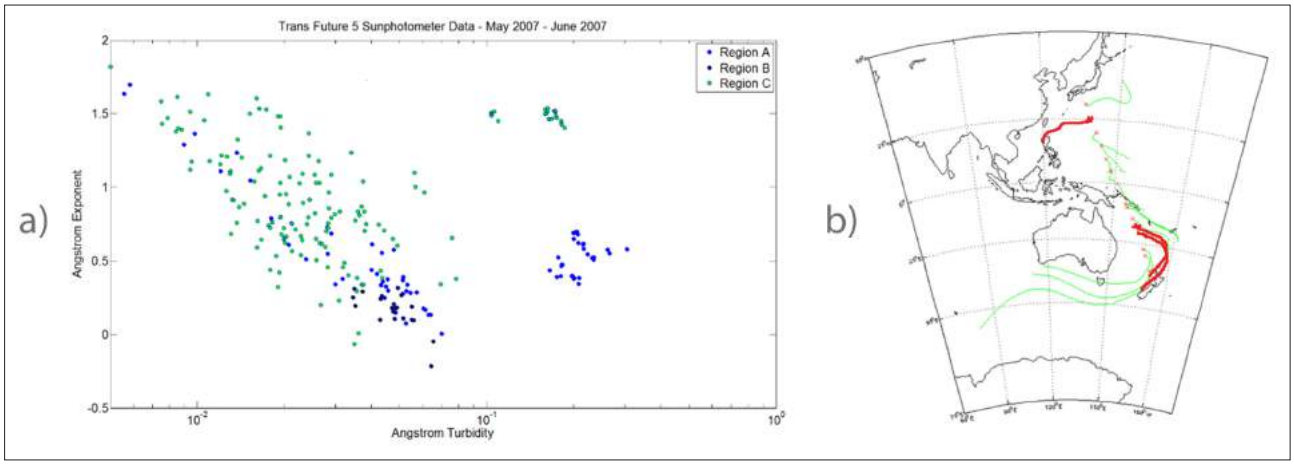

Figure 11: (a) AOD data associated with the May 2007 voyage. (b) May 2007 voyage back trajectories. Trajectories in red indicate air that has passed over large urban areas.

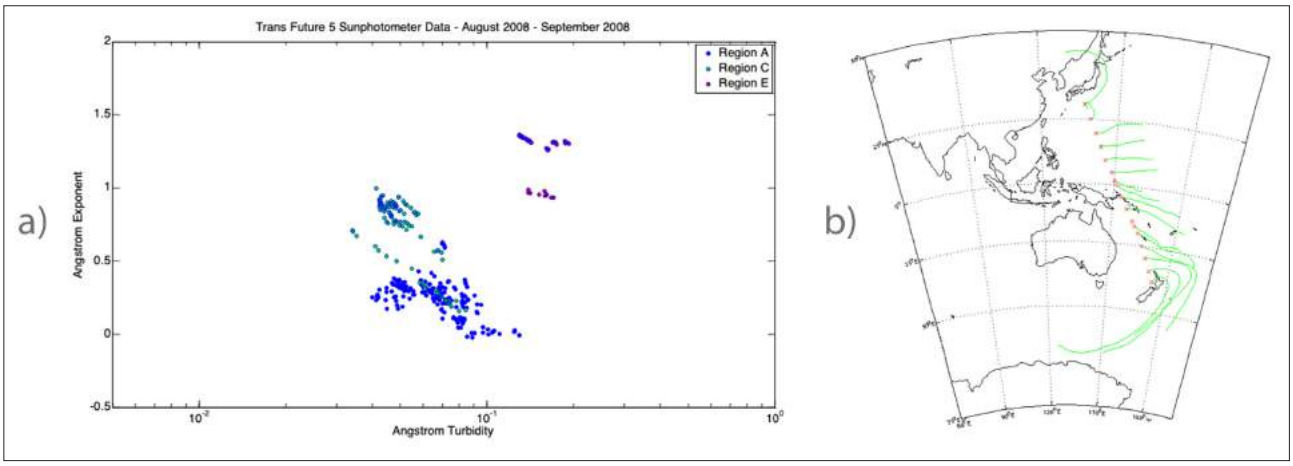

Figure 12: (a) AOD data associated with the September 2008 voyage. (b) September 2008 voyage back trajectories.

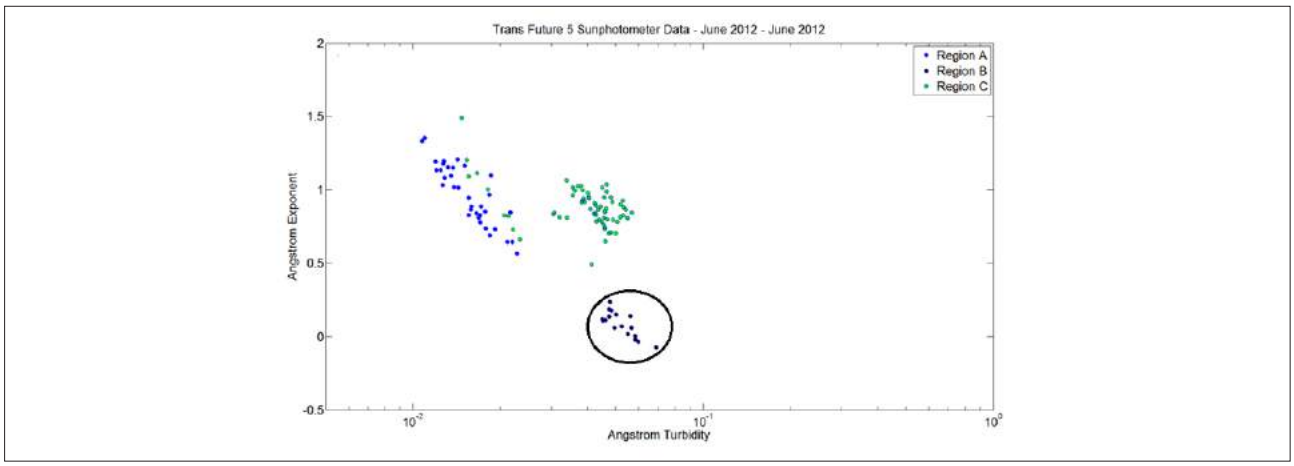

Figure 13: AOD data associated with the June 2012 voyage. The circled values indicate particles from a mineral dust source and coincide with the trajectories off Australia plotted in Fig.6.

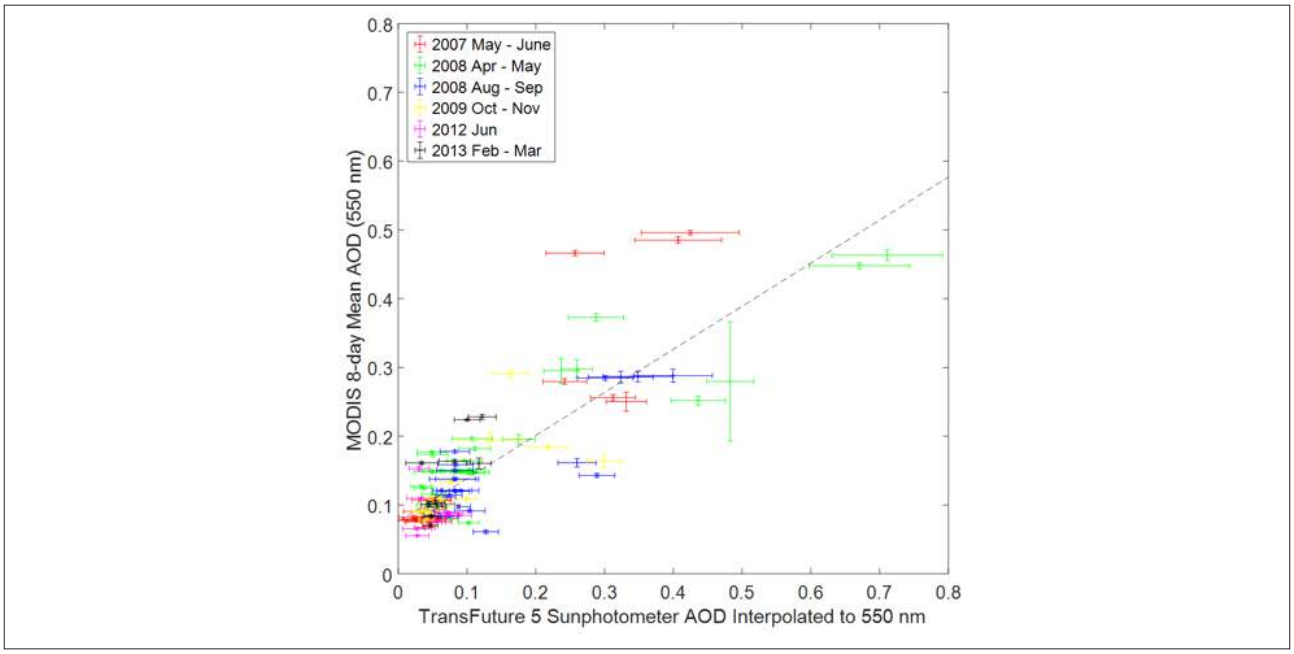

Figure 14: Transfuture5 sunphotometer data and MODIS satellite AOD data comparison.

the Moderate Resolution Imaging Spectroradiometer (MODIS) instrument flown on board the Aqua spacecraft. Aqua is in a sun-synchronous polar orbit at 705km altitude and a 98 minute period, giving global coverage. Any given point on Earth's surface will have approximately two overpasses each day.

In Figure 14, the Transfuture5 sunphotometer AOD data are compared with Aqua MODIS 8-day mean AOD. Over-ocean intercomparisons between individual MODIS images and the MAN system data are significantly constrained by the limited temporal sampling and coverage available from shipboard measurements. As the shipboard sunphotometer measurements times and locations were not chosen to coincide with Aqua overpasses, 8-day mean rather than individual MODIS AOD images were used to compensate for the lack of precise spatial and temporal co-location.

The shipboard sunphotometer measurements were grouped according to which MODIS image pixel (1°longitude x 1°latitude) they were located in; then for each pixel the sunphotometer AOD data were interpolated to the MODIS wavelength (550nm) by least squares fitting the Angstrom relation to the individual measurements. The corresponding MODIS AOD data for the group was obtained by bi-linear interpolation at the mean location of the sunphotometer group.

The resulting data shown in Figure 14 are colour coded by Transfuture5 voyage. For the MODIS data the uncertainty bars on the points are the standard deviation of the daily mean AOD, and give an indication of the variability of the AOD over the 8-day period. The uncertainty bars for the shipboard sunphotometer data are the 95% confidence limits for the Angstrom relation fit. The MODIS and shipboard sunphotometer data are in general agreement. The linear regression relation for the data is $AOD_{MODIS} = 0.63\ AOD_{TF5} + 0.076$, with a correlation coefficient of 0.85 explaining 72% of the variance.

5. Conclusions

We have presented a set of atmospheric condensation

nuclei (CN) measurements from a series of ship transects across the western Pacific Ocean from Nelson, New Zealand to Osaka, Japan between 2006 and 2013. From 2007 aerosol optical depth (AOD) measurements were made on the voyages, every 20 minutes during daylight hours when the sun was clear of cloud. Information from Hysplit back-trajectory calculations were used to identify aerosol source regions. Five distinct regions were identified: (A) the region of the south Pacific Ocean south of 10°S incorporating the south-east trade wind regime of the South Pacific and on many occasions incorporating air that may also have travelled through the Southern Ocean areas south of Australia before being entrained in the south-east trades flow; (B) the Australian continent; (C) The North Pacific Ocean; (D) south-east Asia, incorporating Indonesia and the Philippine Islands; and finally (E) continental Asia.

Substantial temporal variability in fine spatial structure of the latitudinal occurrence of CN was found. In the equatorial western Pacific Ocean this often reflected the position and strength of the SPCZ and ITCZ. However, CN counts for all voyages followed the same broad pattern: highly variable in the vicinity of New Zealand, with variable and occasionally high counts north of New Zealand as far as the SPCZ and ITCZ. Relatively low but variable counts in the areas of the convergence zones, followed by low counts through the northwest Pacific before increasing in outflow from Japan, Korea and China. These regional differences will likely influence regional differences in both direct and indirect aerosol radiative forcing.

AOD data matches well with the aerosol source regions identified by back trajectory calculations. Direct satellite – ship inter-comparisons of AOD are constrained by the difficulty in obtaining spatially and temporally co-located data. However, there is potential for the combination of satellite remote sensing, surface-based measurements from ships, and back trajectory modelling to shed light on the characteristics, distributions and probable sources of aerosols over the open ocean areas of the Earth.

We conclude that the observations of CN and AOD from the ship transects provide useful snapshots of aerosol concentrations and transport across the western Pacific Ocean. The inter-annual variability in the structure of the latitudinal changes in CN concentration suggest that long-range transport and synoptic scale weather systems are the main driver for the observed variations and that the variability in transport is at least as important as variability in sources in determining the spatial structure of CN across the western Pacific.

Acknowledgements

The authors would like to express our gratitude to the Toyofuji Shipping Company for providing passage and facilities on board Transfuture5, and her captain and crew for welcoming us on board. We also thank Y. Nojiri and Shigeru Kariya of NIES for logistical support. Mr Ross Martin of NIWA collected data on several of the voyages. Shipborne sun photometer measurements were made with the support of Alexander Smirnov though the NASA Maritime Aerosol Network.

Data

Data from the NIES Ships of Opportunity program can be accessed via: http://soop.jp

Aeronet MAN data are available through the on-line data base at: http://aeronet.gsfc.nasa.gov/new_web/maritime_aerosol_network.html

AQUA MODIS aerosol data available via: https://modis-atmos.gsfc.nasa.gov/MOD04_l2/index.html

Transfuture5 CN data available via: ftp://ftp.niwa.co.nz/tropac/MV_Transfuture5_western_pacific_CN_data/

References

Andreae, M.O., 1995. Climate effects of changing atmospheric aerosol levels. In World Survey of Climatology, 16. Future Climates of the World A. Henderson-Sellers, pp.341-392.

Boucher, O., Randall, D., Artaxo, P., Bretherton, C., Feingold, G., Forster, P., Kerminen, V.M., Kondo, Y., Liao, H., Lohmann, U. and Rasch, P., 2013. Clouds and aerosols. In Climate change 2013: the physical science basis. Contribution of Working Group I to the Fifth Assessment Report of the Intergovernmental Panel on Climate Change (pp. 571-657). Cambridge University Press.

Charlson, R.J., Lovelock, J.E., Andreae, M.O., & Warren, S.G., 1987. Oceanic phytoplankton, atmospheric sulphur, cloud albedo and climate. Nature 326 pp. 665-661.

Clarke, A.D., and Kapustin, V.N, 2002. A Pacific Aerosol Survey. Part I: A decade of data on particle production, transport, evolution, and mixing in the troposphere. Journal of Atmospheric Sciences, 59(3), pp. 363-382.

de Leeuw, G., Guieu, C., Arneth, A., Bellouin, N., Bopp, L., Boyd, P.W., Denier van der Gon, H.A.C., Desboeufs, K.V., Dulac, F., Facchini, M.C., Gantt, B., Langmann, B., Mahowald, N.M., Marañón, E., O'Dowd, C., Olgun, N., Pulido-Villena, E., Rinaldi, M., Stephanou, E.G., Wagener, T., 2014 Ocean–Atmosphere Interactions of Particles. In: P.S.Liss and M.T. Johnson (Eds). Ocean-Atmosphere Interactions of Gases and Particles. Springer Earth System Sciences: pp. 171-246. doi: 10.1007/978 3 642 25643 1_4

Draxler, R.R. and Rolph, G.D., 2003. HYSPLIT (Hybrid Single-particle Lagrangian Integrated Trajectory) Model, NOAA Air Resources Laboratory, Silver Spring, MD. Access via NOAA ARL READY Website: https://www.ready.noaa.gov/index.php

Ehhalt, D., Zellner, R., Georgii, H.W., Warneck, P., Zellner, R., Mentel, T.F. and Sausen, R., 1999. Global Aspects of Atmospheric Chemistry (Vol. 6). Springer Science & Business Media.

Ekström, M., McTainsh, G.H., Chappell, A., 2004. Australian dust storms: temporal trends and relationships with synoptic pressure distributions (1960–99). International Journal of Climatology, 24(12), pp. 1581-1599

Fitzgerald, J.W. 1991. Marine aerosols: A review. Atmospheric Environment. Part A, General Topics, Volume 25 (3), pp. 533-545.

Hoppel, W. A., Fitzgerald, J. W., Frick, G. M., and Larson, R. E., 1990. Aerosol size distribution and optical properties found in the marine boundary layer over the Atlantic Ocean, Journal of Geophysical Research: Atmospheres, 95(D4), pp.3659-3686.

Kainay,E. and Coauthors, 1996: The NCEP/NCAR Reanalysis 40-year Project. Bulletin of the American Meteorological Society, 77, pp 437-471.

Loewe, F., 1943. Dust storms in Australia. Commonwealth Meteorological Bureau Bulletin, No. 28, Melbourne.

Martino, M., Hamilton, D., Baker, A.R., Jickells, T.D., Bromley, T., Nojiri, Y., Quack, B., and Boyd, P.W., 2014. Western Pacific atmospheric nutrient deposition fluxes, their impact on surface ocean productivity. Global Biogeochemical Cycles 28 (7), pp. 712-728.

McNaughton, C.S., Clarke, A.D., Howell, S.G., Moore, K.G., Brekhovskikh, V., Weber, R.J., Orsini, D.A., Covert, D.S., Buzorius, G., Brechtel, F.J., Carmichael, G.R., Tang, Y., Eisele, F.L., Mauldin, R.L., Bandy, A.R., Thornton, D.C., Blomquist, B., 2004. Spatial distribution and size evolution of particles in Asian outflow: Significance of primary and secondary aerosols during ACE-Asia and TRACE-P. Journal of Geophysical Research: Atmospheres, 109(D19). doi:10.1029/2003JD003528

Merrill, J. T., Uematsu, M., and Bleck, R., 1989. Meteorological analysis of long range transport of

mineral aerosols over the North Pacific. Journal of Geophysical Research: Atmospheres, 94(D6), pp.8584-8598.

Merrill, J.T., Newell, R.E., and Bachmeier, A.S., 1997. A meteorological overview for the Pacific Exploratory Mission – West, Phase B. Journal of Geophysical Research: Atmospheres, 102(D23), pp.28241-28253.

Nara, H., Tanimoto, H., Nojiri, Y., Mukai, H., Machida, T., and Tohjima, Y., 2011. Onboard measurement system of atmospheric carbon monoxide in the Pacific by voluntary observing ships. Atmospheric Measurement Techniques, 4(11), pp.2495-2507.

O'Loingsigh, T., Chubb, T., Baddock, M., Kelly, T., Tapper, N.J., De Deckker, P., McTainsh, G., 2017. Sources and pathways of dust during the Australian "Millennium Drought" decade. Journal of Geophysical Research: Atmospheres, 122(2), pp.1246-1260.

Porter, J.N., Miller, M., Pietras, C., and Motell, C., 2001. Ship-based Sun Photometer Measurements Using Microtops Sun Photometers. Journal of Atmospheric and Oceanic Technology, 18(5), pp. 765-774.

Prospero, J.M., Charlson, R.J., Mohnen, V., Jaenicke, R., Delaney, A.C., Moyers, J., Zeller, W., & Rahn, K,1983. The atmospheric aerosol system – An overview. Reviews of Geophysics and Space Physics, 21(7), pp.1607-1629.

Prospero, J. M., M. Uematsu, and D. L. Savoie,, 1989. Mineral aerosol transport to the Pacific Ocean. In Chemical Oceanography, 10, pp.188– 218.

Smirnov, A., Holben, B.N., Slutsker, I., Giles, D., C.R., M., Eck, T.F., Sakerin, S.M., Macke, A., Croot, P., Zibordi, G., Quinn, P., Sciare, J., Kinne, S., Harvey, M., Smith, T., Piketh, S., Zielinski, T., Proshutinsky, A., Goes, J., Siegel, D.A., Larouche, P., Radionov, V.F., Goloub, P., Krishnamoorthy, K., Mataresse, R., J., R.E., Jourdin, F. 2009. Maritime Aerosol Network (MAN) as a component of AERONET. Journal of Geophysical Research, [Atmospheres], 114: D06204. doi: 10.1029/2008JD011257.

Smirnov, A., Holben, B.N., Giles, D.M., Slutsker, I., O'Neill, N.T., Eck, T.F., Macke, A., Croot, P., Courcoux, Y., Sakerin, S.M., Smyth, T.J., Zielinski, T., Zibordi, G., Goes, J.I., Harvey, M.J., Quinn, P.K., Nelson, N.B., Radionov, V.F., Duarte, C.M., Losno, R., Sciare, J., Voss, K.J., Kinne, S., Nalli, N.R., Joseph, E., Krishna Moorthy, K., Covert, D.S., Gulev, S.K., Milinevsky, G., Larouche, P., Belanger, S., Horne, E., Chin, M., Remer, L.A., Kahn, R.A., Reid, J.S., Schulz, M., Heald, C.L., Zhang, J., Lapina, K., Kleidman, R.G., Griesfeller, J., Gaitley, B.J., Tan, Q., Diehl, T.L. 2011. Maritime aerosol network as a component of AERONET – first results and comparison with global aerosol models and satellite retrievals. Atmos. Meas. Tech., 4(3): pp. 583-597. doi: 10.5194/amt-4-583-2011.

Vincent, D.G., 1994. The South Pacific Convergence Zone (SPCZ): A Review. Monthly Weather Review, 122, pp.1949-1970.

Zaizen, Y, Ikegami, M., Tsutsumi, Y., Makino, Y., Okada, K., Jensen, J., and Gras, J.L., 1996. Number concentration and size distribution of aerosol particles in the middle troposphere over the Western Pacific Ocean. Atmospheric Environment, 30(10-11), pp.1755-1762.